Flyover noise evaluation of low-noise technologies applied to a blended wing body aircraft

Ingrid LeGriffon[1]
Office National d'Études et de Recherches Aérospatiales (ONERA) – Paris Saclay University
92322 Châtillon Cedex, France

Lothar Bertsch[2]
German Aerospace Center (DLR)
37073 Göttingen, Germany

Francesco Centracchio[3]
Università degli Studi Roma Tre, Dipartimento di Ingegneria
00146,Rome, Italy

Daniel Weintraub[4]
RWTH Aachen University, Institute of Jet Propulsion and Turbomachinery
52062 Aachen, Germany

ABSTRACT

In the frame of the European research project ARTEM (Aircraft noise Reduction Technologies and related Environmental iMpact), new aircraft architectures and alternative propulsion systems, e.g. Blended Wing Body (BWB) and geared turbofan engine concept, are investigated, as well as innovative noise reduction technologies such as metamaterials and low noise high-lift device systems. A noise impact assessment has been performed on a long-haul BWB concept developed by Roma Tre University, using the System Noise Prediction Tools of ONERA (CARMEN) and DLR (PANAM). First, shielding effects on the main noise emission sources are discussed, through installation effects hemi-spheres at relevant third-octave band frequencies around the aircraft. Based on the shielding assessment, detailed take-off and landing procedures are simulated for several aircraft configurations. Two alternative motorisations of the BWB are evaluated (BPR 8 and BPR 12), provided by RWTH Aachen. Finally, the most promising low noise technologies developed in the frame of ARTEM are applied, and their impact on the aircraft's overall noise levels on the ground is discussed. It can be demonstrated how the specific aircraft configuration, the engine type and the additional low-noise technology result in a significant overall noise reduction. An accompagning conference paper presents flyover auralisations based on these total aircraft noise calculations.

[1] ingrid.legriffon@onera.fr
[2] lothar.bertsch@dlr.de
[3] francesco.centracchio@uniroma3.it
[4] weintraub@ist.rwth-aachen.de

1. INTRODUCTION

New aircraft concepts are essential if relevant reduction of aircraft noise is a goal. It has been demonstrated in the past that conventional aircraft concepts cannot even reach the H2020 goals, even if equipped with low-noise technology [1]. Consequently, novel designs and concepts are required. In this perspective, the H2020 project ARTEM (for **A**ircraft noise **R**eduction **T**echnologies and related **E**nvironmental i**M**pact) was launched, with the goal to develop novel aircraft configurations for 2035 and 2050, investigate noise sources relative to these new concepts and apply additional technology to further reduce the noise received on the ground. In this project, the authors of this paper participated in the development of novel technologies, the aircraft design, the flight simulation, the engine design, and of course the overall noise prediction. This paper summarizes the results of the evaluation of a 2050 Blended Wing Body with novel technology as developed within ARTEM.

First, the noise prediction tools used by partners for creating shielding and noise maps are presented. Then, the case study is presented, with the description of the aircraft platform and the installed engines. Selected low-noise ARTEM technology is briefly introduced and the assumed impact on certain component's noise emission are documented. Finally, shielding effects (due to the very particular aircraft geometry) and noise footprints for the overall aircraft along departure are presented. The presented ground noise results are limited to the assessment of A-weighted Sound Pressure Levels and Sound Exposure Level.

2. SYSTEM NOISE PREDICTION TOOLS

Two system noise prediction tools were used for this case study: Onera's in-house tool CARMEN, combined with a Boundary Element Method (BEM) / Integral Method solver, and DLR's PANAM connected to a ray-tracer with integrated diffraction correction referred to as SHADOW.

2.1. ONERA tool chain

Over the last decade efforts were made at ONERA to develop a parametric tool, based on simple models, which would be able to predict the noise footprint of an aircraft flyover. This tool, CARMEN, has served for parametric evaluation of new aircraft concepts [2] for the last few years. It is based on three modules: the calculations of noise emission sources, the installation effects and the propagation through the atmosphere to the receiver.

The main noise emission sources encountered on a classical tube and wing aircraft and a rotorcraft are implemented. They are mainly based on semi-empirical and semi-analytical formula. Strong hypotheses are made to simplify calculations. Noise sources are considered point sources and the semi-empirical models provide directivity and spectra in the far field. Near field acoustic installation effects are therefore (not yet) taken into account.

CARMEN models every noise individually for each time step of the aircraft flight trajectory and then sums them up, taking into account their installation on the aircraft. Masking, reflection, and diffraction are either calculated by BEM or a simplified integral method. These calculations are done beforehand, taking into consideration the aircraft geometry and the point source location. A pattern is calculated for each source location and frequency and fed into CARMEN to add to the source directivities and spectra. The use of BEM is generally bound to low and medium frequencies due to expensive computational time. For higher frequencies, a simplified integral method is used. The proposed method relies on the Kirchhoff approximation [3] to solve scattering problems by means of the Kirchhoff-Helmholtz equation defined on the scattering object surface. For now, only first reflections are considered. In order to take into account diffracted waves, we use the Maggi-Rubinowicz formulation of the Kirchhoff diffraction theory, similarly to Lummer [4].

The atmospheric propagation to the ground is then dealt with by applying a ray tracing technique, including atmospheric absorption, geometric attenuation and Doppler and flight effects. Meteorological conditions such as wind and temperature profiles can be included. After propagation, one obtains noise spectra at every pre-defined receiver position, for every noise source, at every time step of the simulated aircraft trajectory.

2.2. DLR tool chain

DLR is applying its internal software PANAM [5]. Similar to CARMEN, the code is comprised of individual algorithms that each describe the noise generation of a specific noise emission source or interaction effect. The models are semi-empirical and parametric, i.e., accounting for modifications to both geometry of aircraft end engine but also to the operation of the aircraft. Similar as for CARMEN, such a setup enables the prediction of aircraft noise along arbitrary flight procedures. Underlying simplifications and also limitations of the applied models are comparable to CARMEN (cf. chapter 2.1).

For the noise shielding assessment of the different noise sources, the DLR code SHADOW is applied as described in Lummer [4]. In contrast to ONERA's approach, this method is adapted to be applicable to the entire frequency range of interest, i.e., the same method is validated for low and high frequencies. Similar to the ONERA approach, delta levels are predicted for each selected noise source, e.g., landing gear, and then superimposed on the predicted source emission according to the implemented noise source models. Such a delta level is then stored for each emission angle and for each third-octave band frequency in so called emission hemi-spheres.

2.3. Comparison of methods

The implemented methods and the general work flow of both tools are assessed in more detail in Ref. [6] and prediction results are directly compared. Furthermore, the NASA prediction software ANOPP has been included into this earlier comparison. Although the predictions have been based on similar input, certain differences in predicted source noise levels have been documented among the three tools. The remaining differences have been either attributed to different models for a specific noise emission source, have been attributed to implementation differences for certain models, or are caused by each organizations individual and specific tool work-flow. Discovered prediction differences typically are within a 3 dB margin for conventional tube-and-wing aircraft. If noise shielding effects are prevailing, somewhat larger differences and discrepancies (most often also within 3 dB) can be observed caused by the different shielding tools.

The discrepancies in results shown in the earlier tool benchmark [6] are in good agreement with parallel research activities conducted by DLR and Empa on underlying simulation uncertainties [7,8] for the noise emission models as applied by ONERA and DLR in their codes CARMEN and PANAM, respectively. The simulation uncertainties for immission levels are furthermore strongly dependent on the current operating conditions along the flight path, the modeling of the ground attenuation, and on the receiver distance due to prevailing propagation effects. Obviously, immission levels are associated with additional uncertainty compared to the emission situation assessment. Further differences have to be expected whenever noise shielding effects are affecting the dominant noise sources since it has been shown that shielding predictions by the different tools result in discrepancies. A better agreement of the prediction results than what has been shown in Ref. [6] can therefore not be expected; especially not for such an unconventional and novel concept as studied in this paper. Furthermore, landing gear and jet have been evaluated for shielding effects as well, for which the use of PANAM has not been subject to in previous assessments. Consequently, it has to be expected to see differences in the predicted immission levels by the two tool chains. Any too close agreement would be purely coincidental.

3. TEST CASE SET – UP

3.1. BOLT aircraft

The BOLT (Blended wing body with Optimized Low-noise Technologies) configuration is one of the three Blended Wing Body (BWB) layouts developed within the ARTEM project by Roma Tre University. The configuration meets the requirements of a long-haul modern aircraft, with an expected payload of 400 passengers in a two-classes cabin layout: the design mission consist of 5500 nmi range with a flight speed of 510 knots at 43 kft and is equipped with two last-generation turbofan engines.

The initial layout was derived based on the experience acquired by the research group over the past years using the in-house MCRDO (Multidisciplinary Conceptual Robust Design Optimisation) framework FRIDA (FRamework for Innovative Design in Aeronautics), developed by the Aerospace Structures and Design group of Roma Tre University [9]. The tool FRIDA is capable to deeply describe the aircraft from a multidisciplinary point of view, and is suitable for all those applications that require the aircraft configuration definition, the environmental impact estimation [10] combined with financial metrics [11,12]. It must be pointed out that FRIDA was developed to assess the conceptual design of both conventional and innovative aircraft [13], thus the employed algorithms are, whenever possible, prime-principle based. Specifically, the preliminary weight breakdown is carried out using validated semiempirical techniques in addition to the inner layout definition; the isolated wing structural analysis makes use of an in-house Finite Element Method solver starting from an equivalent beam; the aerodynamic assessment is performed using a zero-th order boundary element solution of the integral equation for quasi-potential flows, and suitable corrections are applied to account for viscosity, compressibility and transonic effects; the performance analysis ensures the correct flight properties in terms of attitudes for each mission phase, ground distances, as well as stall speeds.

The BOLT optimised layout has been obtained within FRIDA using a multilevel approach to reduce the domain size. Below, in a synthesis of the achievements in terms of maximum takeoff weight (MTOW), average cruise efficiency (avg Lift/Drag L/D) and maximum aerodynamic efficiency (max L/D) are reported in Table 1.

Table 1 : Synthesis of the optimisation achievements for the BOLT layout

	MTOW	**avg L/D**	**max L/D**
Initial Layout	230 ton	20,5	20,8
Optimised Layout	223 ton	22	23,0
Improvement	-3%	+7,3%	+10,5%

3.2. BPR 8 and BPR 12 engine data

Two turbofan engines have been predesigned, featuring design bypass ratios of 8 and 12. These are referred to as the BPR8 and BPR12 engines. The software GasTurb [14] was used for the design (sizing) and off-design (performance analysis) calculations, to provide the thermodynamic and geometric input data for the noise assessment. The general approach to engine preliminary design and modeling is described in detail in [15], and only summarized here for both engines along with the key design parameter choices. The engines are designed as two-spool geared turbofans with separate, non-variable, core and bypass nozzles. A top of climb operating point has been selected as engine design point, at 43 kft and 0.84 flight Mach number. Following current trends in the field of high bypass turbofan engines, an overall pressure ratio of 60 and a burner exit temperature of 1700 K have been set for the design point. Component efficiencies were evaluated with the correlations available in GasTurb [14]. Fan pressure ratio and engine mass flow were selected to achieve a design point net thrust of 70 kN, along with the target bypass ratios. An inlet Mach number of 0.68 has been selected, which then yields fan diameters of 3.25 m (BPR 8) and 3.75m (BPR 12). The resulting preliminary design cross sections are shown in Figure 1. The design point SFC is 14.71 and 13.95 g/kNs for the BPR 8 and BPR 12 engines, respectively. For off-design calculations, GasTurb uses scaled compressor and turbine maps, which in this work were taken from [16]. GasTurb Dynamic Linked Libraries (DLLs) were employed to automatically evaluate engine performance over a broad range of operating conditions for the purpose of mission performance analysis. The output data includes cross sections and blade numbers, spool speeds as well as mass flows, pressures and temperatures at the engine's thermodynamic stations.

At this point it should be noted, that the GasTurb software is capable of deriving all the required input parameters for an overall engine noise prediction performed by the DLR and ONERA software in an adequate level of fidelity. Certain parameters of the engine performance have a strong impact on the noise prediction, e.g., jet exhaust velocities, and an adequate level of fidelity is essential to ensure realistic and reliable results.

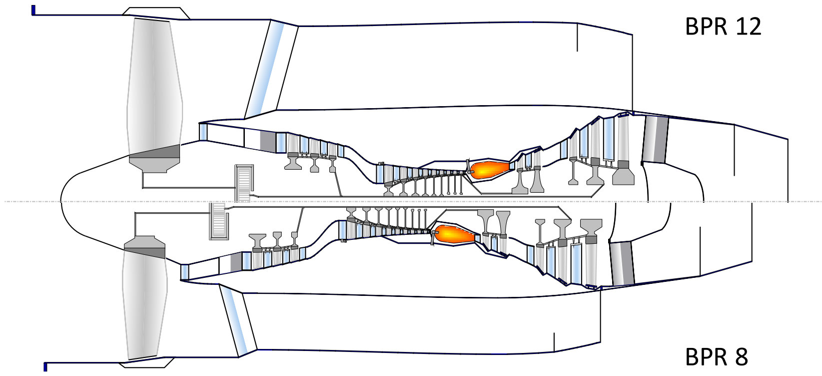

Figure 1: Turbofan engine preliminary designs (BPR 8 and BPR 12)

3.3 Low Noise Technologies

In addition, low noise technologies (LNT) developed and studied by ARTEM partners (publications to come) were translated into noise deltas and "added" to the BOLT noise source predictions. For an initial assessment as presented in this paper, no potentially disadvantageous (but minor) effects on flight performance or engine performance have been accounted for.

For this application, low noise technologies were evaluated as a package, and not individually. This package includes fan inlet and outlet lining, a new trailing edge technology, jet porous material and a main landing gear noise reduction. Except for the landing gear noise (constant value), all LNTs are frequency dependent, but constant in directivity. The delta dB values that are added to every individual noise emission source during the flyover noise calculations are presented in Table 2. Negative values signify a level increase.

Table 2 : LNT induced noise delta in dB, applied to each considered noise source, as a function of frequency

Frequency [Hz]	Fan liner (front and rear) Δ dB	Trailing edge device Δ dB	Porous jet material Δ dB
20 - 200	0	6	2
250 - 315	3	6	2
400	4	6	2
500	5	6	2
630	8	6	2
800	18	8	2
1000	12	10	2
1250	8	7	-1
1600	2	7	-1
2000 - 5000	0	7	-1
6300 - 20000	0	5	-1

4. SHIELDING EFFECTS

As a first step in the aircraft evaluation, the shielding effects of the aircraft architecture were considered, without any specific source directivities. The aircraft mesh was delivered by UniRoma3 (UR3) and readapted by the research partners to fit their installation effects calculation codes. Five distinctive noise sources are considered: jet, fan inlet, fan outlet, main landing gear and nose landing gear. Their positions on the aircraft were chosen as shown in Figure 2. They were based on geometric assumptions of the engines. In order to keep results comparable between partners, it was decided to use single radiating monopoles at the source location.

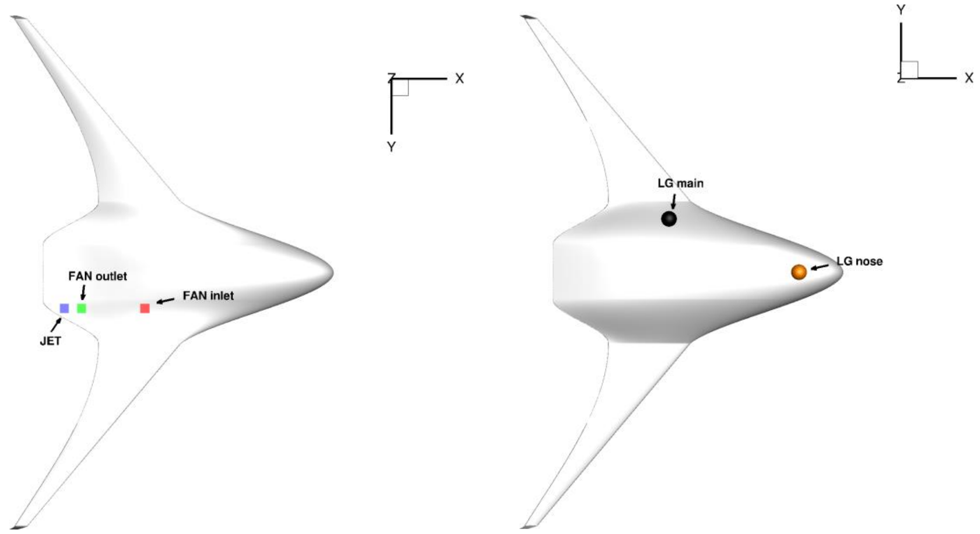

Figure 2: Sources locations on the BOLT configuration, engines installed over the wing

In the following, all installation effects computations have been performed for one source location on the right side of the aircraft at a time for all third octave band central frequencies up to 10 kHz. The results for the sources on the left side of the aircraft were obtained by symmetry and are summed afterward with their symmetric counterpart as an incoherent summation. This is based on the hypothesis that real sources are not perfectly in sync with each other and thus considering a coherent summation would introduce a bias. All shielding factors for each third octave band centre frequencies are assessed and later on accounted for in the system noise prediction process by DLR and ONERA, respectively.

Representative shielding maps were extracted at two frequencies: 250 Hz and 1000 Hz. These two frequencies were chosen as representative center band frequencies for fan noise and airframe noise contribution which seem of utmost importance for the BOLT vehicle. Furthermore, the two different frequencies are of increased interest because of the different simulation approaches used by ONERA to generate them (Boundary Element Method for 250 Hz, simplified integral method (see 3.1) for 1000 Hz). DLR's SHADOW tool is directly applied for the full spectral range.
The following figures gather the two partners' results for both frequencies, each figure representing one source location (+ its symmetry). The shown attenuation number are the values to be added to levels which would have been obtained without the aircraft geometry influence. Positive values therefore indicate a level increase, negative values indicate masking and level reduction.

For the fan inlet source location (Figure 3), both partners show very similar shielding patterns. A clear noise masking towards the ground is observed while levels start to increase at level of the aircraft plane and higher. Higher frequencies show higher noise reduction below the aircraft.

Fan outlet and jet (Figure 4) show very similar patterns due to very closely located source locations. It has to be reminded that this is an academic study, where the jet noise source is considered a point source. Although this is a simplified, not realistic source representation it enables an easier direct comparison between partners. Both tools show a clear masking towards to front of the aircraft while aft angles see an increase of at least 2 dB for both partners.

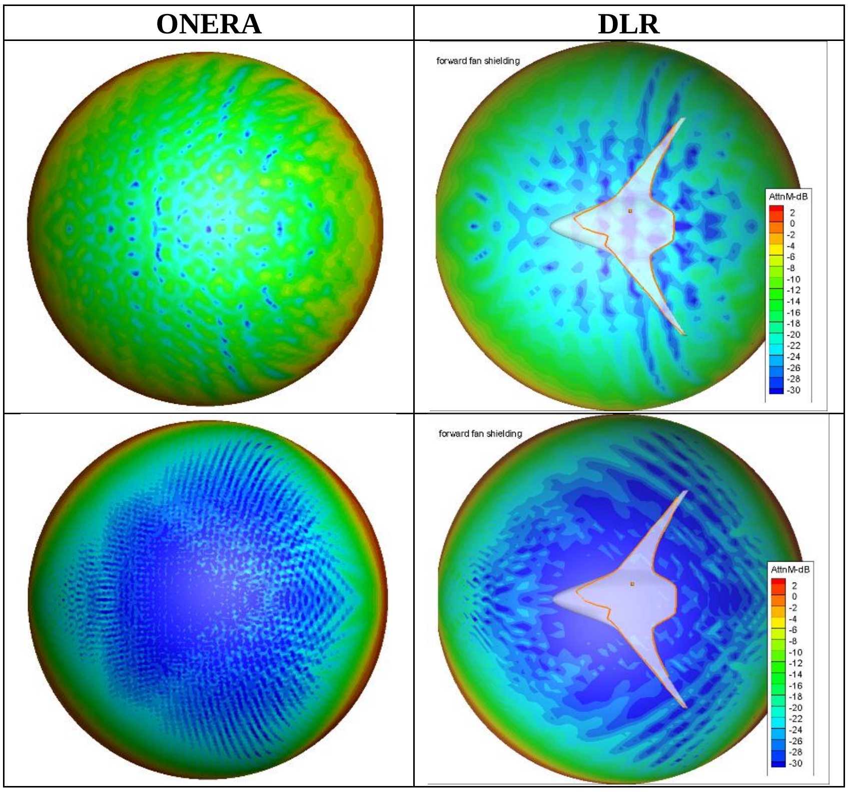

Figure 3 : Fan inlet shielding – 25 Hz (above) and 1000 Hz (below)

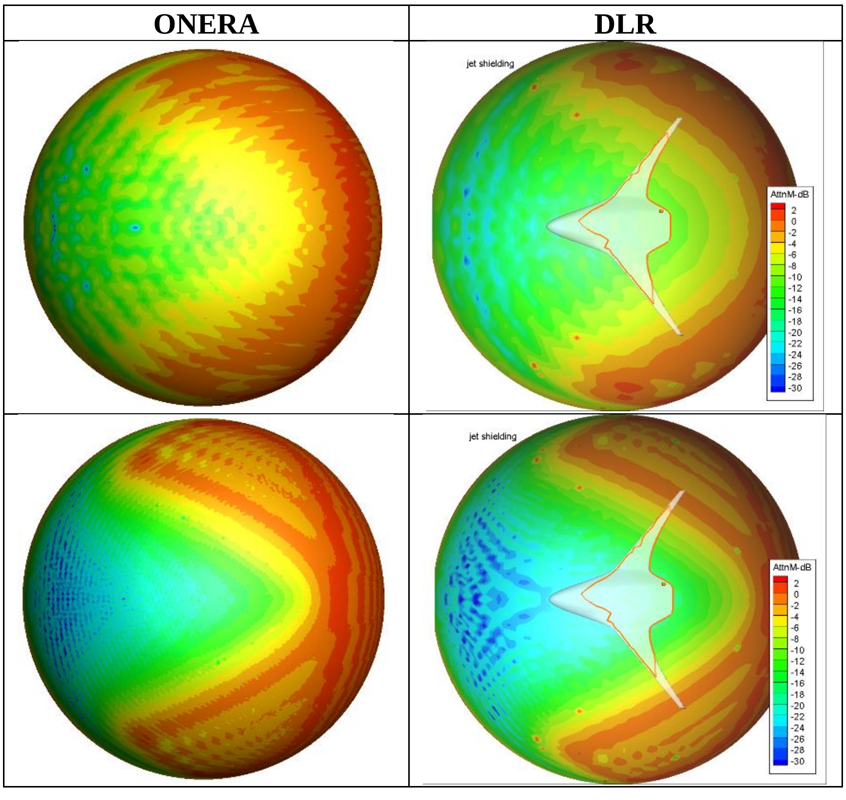

Figure 4 : Jet shielding – 250 Hz (above) and 1000 Hz (below)

The position of fan exhaust and jet noise source close to the trailing edge leads to much smaller shadow zones below the aircraft, than what can be seen for the fan inlet noise source position. For the fan outlet and the jet shielding, ONERA and DLR results are in very good agreement, i.e., level and directivity. The differences are reduced compared to the inlet shielding due to simplified shielding surface to the back, i.e., effect of sharp leading edges.

Since landing gears are located below the aircraft, a general increase due to reflections is expected towards the ground. Indeed, for the main landing gears (Figure 5) high reflections and interactions leading to localized noise reductions can be seen in the ONERA and DLR results.

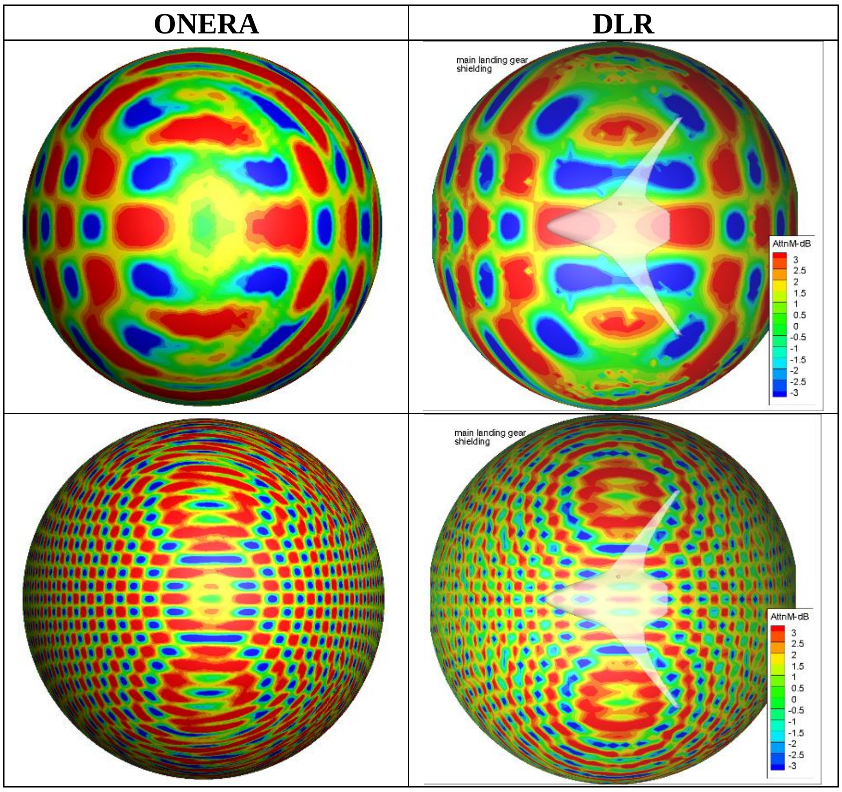

Figure 5 : Main landing gear shielding – 250 Hz (above) and 1000 Hz (below)

A general conclusion can be that for engine noise sources levels an increase can be observed at aft angles, to the back of the aircraft, while front angles see a potentially high masking effect. This effect should be visible on time level histories on the ground, when the aircraft flies over the microphone. It should be noted that the shielding effects for the landing gear result in an amplification of levels due to reflection at the wing.

5. NOISE ASSESSMENT

5.1 Case studies

The next step in the aircraft evaluation consists in doing whole system noise predictions, i.e. calculating the noise radiated by the aircraft over an entire flight procedure. Among other configurations, take-off and landing were assessed for aircraft equipped with the engine types presented in 3.2 and the low noise technologies presented in 3.3.

Flight trajectories and corresponding dynamic engine data were delivered by UR3. All the trajectories have been calculated using the flight simulation environment within the FRIDA framework, and the implemented technique is based on the inverse flight mechanics: once the trajectory kinematics is known, the equilibrium of the forces is imposed: thus, the reference angle of attack and the thrust are evaluated in order to ensure the airworthiness, also accounting for the static longitudinal stability. Downstream the trajectory calculation, the relevant engine data are estimated in FRIDA using a simple but effective semiempirical model. The model, starting from the flight condition and the engine features, provides the rotational speeds N1 and N2 (of respectively low–pressure and high–pressure spools) knowing the overspeed and idle conditions: mass flows, temperatures, pressures and other thermodynamic variables are calculated, based on the fundamental physics and some additional data, as a function of the flight condition and the rotational speeds.

Takeoff and landing configurations were evaluated at pseudo-certification microphone positions (see Figure 6). That is to say 2300 meters before touch down for the approach configuration and 6500 after break release for take-off; both below the flight path. The term "pseudo-certification" is used since no effort was made to satisfy regulatory conditions on flight trajectory and aircraft settings.

In this paper it was decided to focus on takeoff configurations only. The takeoff was selected in order to assess the different engine options and the effectiveness of additional low-noise modifications to the engine, i.e., fan lining and jet exhaust modifications.

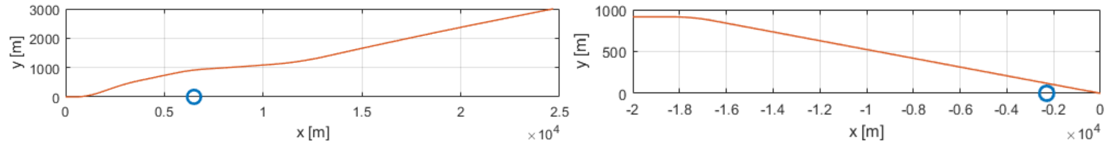

Figure 6 : Takeoff and landing trajectories with associated microphone position

5.2 Results

In the following, calculation results including jet, fan, flap and landing gear noise are presented. All flyovers are calculated taking into account the aircraft shielding effects. Propagation is done through standard atmosphere and no ground effects are taken into account.

First of all, as could be guessed with Figures 3 to 5, an interesting effect of shielding should be observed on ground noise levels compared to classical tube and wing concepts where noise emission sources are hardly masked by the aircraft. As mentioned in 2.3 we have to expect discrepancies between partners with regard to the impact of shielding. To get a quantifiable idea of this discrepancy, one can look at Figure 7 where are illustrated the dBA level differences in maximum A-weighted sound pressure level ($L_{A,max}$) at the selected receiver locations as indicated in Figure 6.

Delta values are positive and have to be understood as noise reduction. For instance for DLR, the inclusion of the shielding effects (contrary to having « free field » noise emission sourrces) reduces the takeoff maximum noise level on the ground by more than 13 dBA. In contrast to that, ONERA only predicts a 6 dBA noise reduction due to the aircraft's geometry. For the following it has therefore to be kept in mind that shielding has a much higher impact on DLR calculations. In order to rapidly check the similarity of the partners' codes (also done in previous studies (see [6]), a more detailed study (not shown here) has shown that the partners' codes give very similar results when applied to the case studies without including shielding effects ($L_{A,max}$ delta between 0.1 and 2.6 dB depending on the considered noise source). When including shielding effects for a novel tube-and-wing aircraft design with noise shielding effects, differences were in the order of 3 dB in $L_{A,max}$ between the three tools.

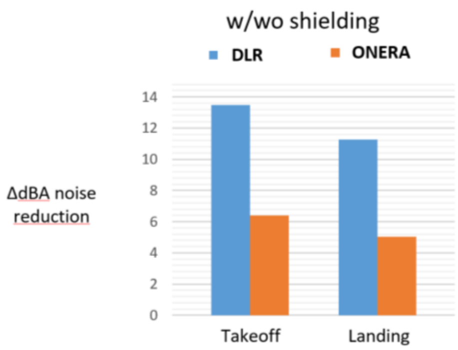

Figure 7 : $L_{A,max}$ noise reduction beetween calculation with and without taking into account shielding effects

Figure 8 shows the impact the aircraft equipment configurations have on $L_{A,max}$ during takeoff at the selected receiver location. Delta dBA are given for comparisons between aircraft with and without LNT (two diagrams to the left), or aircraft equipped with BPR 8 or BPR12 engines (3rd and 4th diagram).

For the first comparison, two aircraft equipped with a BPR8 engine are compared with and without LNT package. For takeoff, the outcome of this comparison is that the choice of adding LNTs to a BPR8 equipped aircraft leads to 3 to 4.5 dBA $L_{A,max}$ reduction (depending on the chosen prediction tool). The effect is slightly higher for a BPR 12 engine equipped aicraft.

The switch from an older (BPR8) to a more recent aircraft engine (BPR12) leads to relatively small noise reductions on the ground for takeoff ($L_{A,max}$ 1-3 dBA, diagrams 3 and 4).

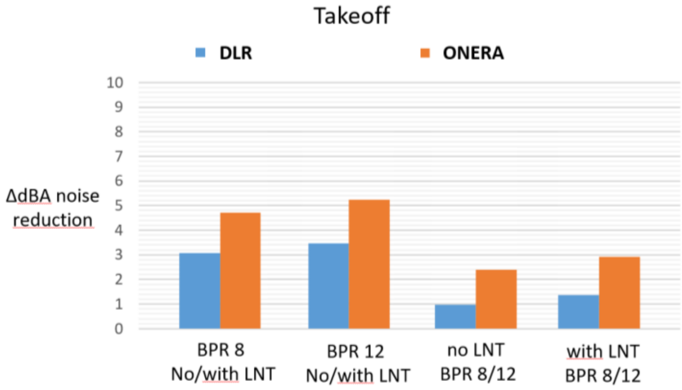

Figure 8: $L_{A,max}$ noise reduction beetween aircraft with and without LNT package (two to the left), and BPR8 and BPR12 configurations (two to the right) for takeoff configurations.

To evaluate the overall noise immission along part of the departure flight, noise contour areas are predicted by both tools and compared. It can be demonstrated, that the benefit of noise shielding will be reduced for receiver locations further away from the flight ground track (Figure 9-10). Despite the differences in noise shielding effectiveness as predicted by both simulation tools, very good agreement can be achieved further away from the flight ground track, i.e., for contours of lower levels.

The predicted A-SEL noise contours are presented in Figure 9 and Figure 10. The simulated area is selected to capture the relevant parts of the departure flight trajectory, i.e., take-off and thrust cut-back. This part of the flight procedure is also relevant for the noise certification of aircraft. Furthermore, prediction results for this area were delivered to EMPA for auralization and a dedicated listening-test under laboratory conditions [17].

In Figure 9 the effect of adding LNT to a BPR 12 engine equipped aircraft is visible. The 70 dBA SEL contours are very close between partners as described above. For higher levels the differences due to the different shielding simulations become dominant and cause visible differences. As a reminder, ± 1 dB difference in the emission prediction can result in up to 40% difference in contour area for typical source distances of an aircraft during departure or final approach [18].

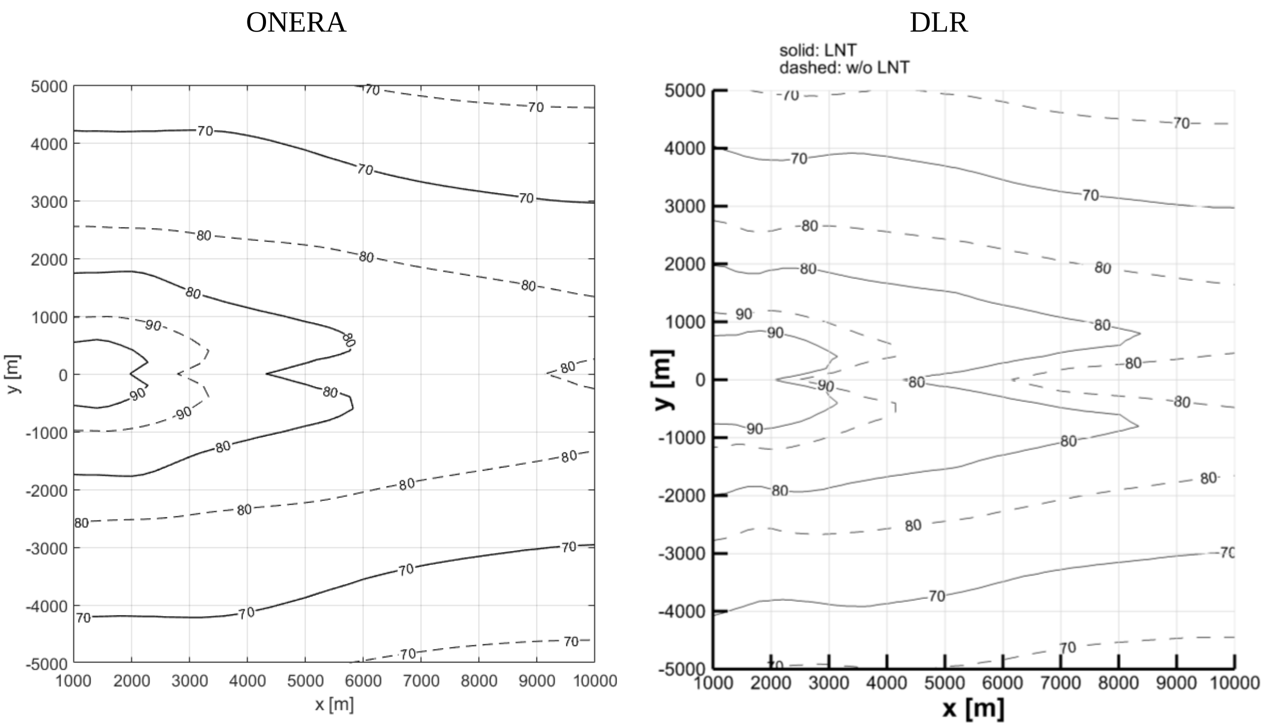

Figure 9 : A-SEL contours for BPR 12 engine equipped aircraft, impact of LNT pakage. Solid line : with LNT, dashed line : without LNT

Figure 10 pictures the effect of upgrading the engine from BPR 8 to BPR 12. The used aircraft here is equipped with the ARTEM LNT package. As already seen in Figure 8 the impact is estimated higher by ONERA than by DLR, probably due to the fact that much of the engine noise contribution is already reduced by stronger shielding according to the DLR calculations.

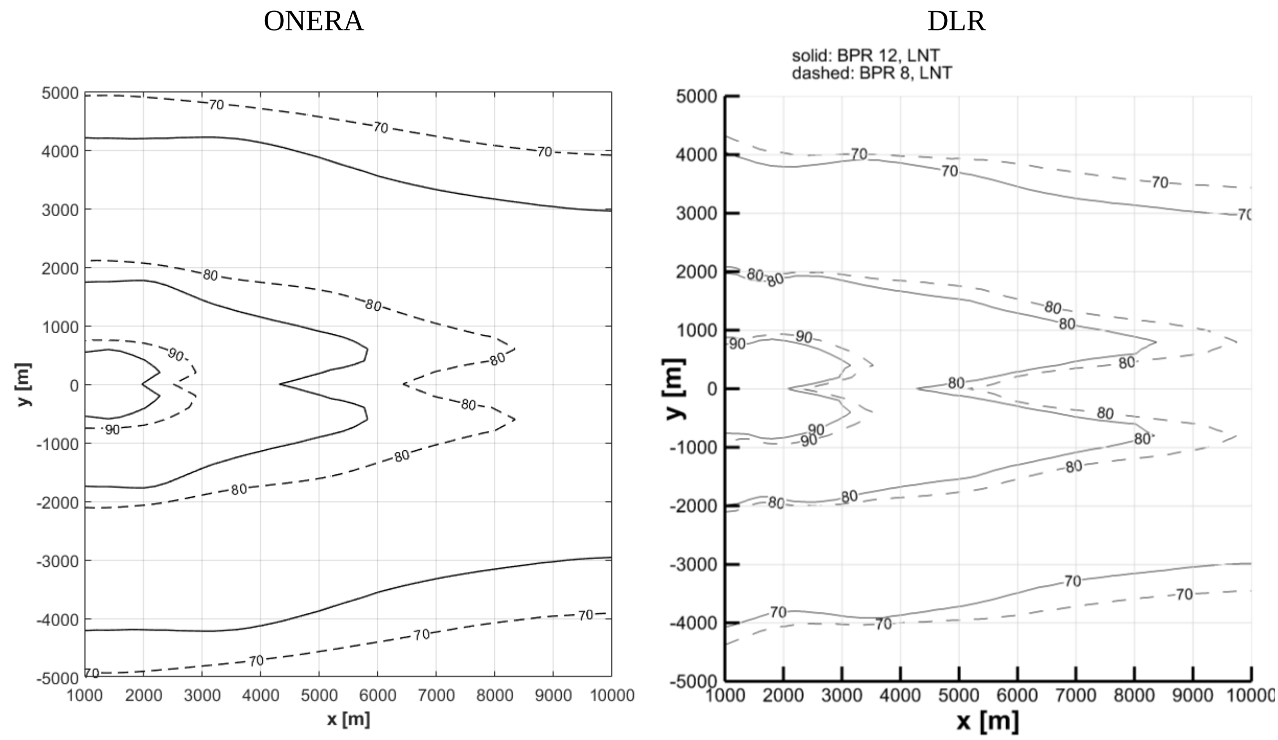

Figure 10 : A-SEL contours for aircraft with LNT, impact of engine choice. Solid line : BPR 8, dashed line : BPR 12

The noise contour areas are predicted under freefield conditions. Consideration of ground attenuation will have a significant impact on the shape of the contours. The presented contours can therefore not directly be compared to simulation results accounting for these effects.

In a general manner one can observe that ONERA estimates bigger noise reduction values through technology change at takeoff than DLR. This is linked to the fact that shielding is higher for DLR than for ONERA (see Figure 7 and 8) which attenuates any influence of engine modifications. The engine replacement yields a significantly larger noise reduction compared to the application of the LNT. Yet, it is demonstrated that the combination of a novel engine concept and the application of LNT is still promising on-board of the ARTEM BOLT vehicle despite and in addition to a significant noise reduction due to shielding effects.

6. CONCLUSIONS

A noise evaluation on the ARTEM Blended Wing Body concept BOLT was performed by ONERA and DLR. In addition to the impact of extreme shielding effects alone, the impact of engine configuration (BPR 8 and BPR 12) was evaluated. Furthermore, a package of low noise technologies developed by ARTEM partners was added to the concept and assessed with regard to its impact on noise levels on the ground. Discrepancies between partners' calculations stayed in the range of previous estimates (due to code implementation, model differences, …). Larger deviations can directly be attributed to differences in the simulation results of noise shielding effects. According to ONERA and DLR predictions, large noise reduction on the ground is achieved through shielding of fan noise on board of the novel BOLT aircraft concept. In addition to that it is demonstrated independently by ONERA and DLR that an engine replacement and the application of the ARTEM LNT will additionally and significantly reduce the total aircraft noise levels along the departure and approach (approach results not shown here).

7. ACKNOWLEDGEMENTS

We gratefully acknowledge the partners of the ARTEM project who delivered the noise delta for low noise reduction technologies, as well as Mathieu Lorteau for the ONERA noise shielding effects calculations. This work received funding from the European Union’s Horizon 2020 research and innovation program within the project ARTEM under the grant agreement no° 769359.

8. REFERENCES

1 Bertsch, L., Simons, D.G. and Snellen, M. (2015) Aircraft Noise: The major sources, modelling capabilities, and reduction possibilities. DLR-Interner Bericht. DLR-IB 224-2015 A 110. 29 S
2 LeGriffon, I., Noise prediction of a new generation aerostat, 26th International Congress on Sound and Vibration, ICSV26, Montréal, Canada, 7-11 July 2019
3 M. Born and E. Wolf, Chapter VIII: Elements of the theory of diffraction, Principles of Optics (Sixth Edition), 1980, pp 370-458
4 M. Lummer, Maggi-Rubinowicz diffraction correction for ray-tracing calculations of engine noise shielding, 14th AIAA/CEAS Aeroacoustics Conference, AIAA 2008-3050, 5-7 May 2008, Vancouver, Canada
5 Bertsch, L; (2013), Noise Prediction within Conceptual Aircraft Design. DLR-Forschungsbericht. DLR-Forschungsbericht 2013-05. Dissertation. Technische Universität Braunschweig. 184 S.
6 Bertsch, L ; Sanders, L ; Thomas, R ; LeGriffon, I ; June, J ; Clark, I ; Lorteau, M ; Comparative Assessment of Aircraft System Noise Simulation Tools, Journal of Aircraft, Vol. 58, No.4, July-August 2021
7 Bertsch, L ; Schäffer, B ; Guérin, S ; Uncertainty Analysis for Parametric Aircraft System Noise Prediction, Journal of Aircraft, Journal of Aircraft, Vol. 56, No.2, March-April 2019
8 Römer, U ; Bertsch, L ; Mulani, S.B ; Schäffer, B ; « Uncertainty Quantification for Aircraft Noise Emission Simulation: Methods and Limitations », AIAA Journal, Vol.60, No.5, May 2022
9 Knobloch, K.; et al., Future Aircraft and the Future of Aircraft Noise. In Aviation Noise Impact Management: Technologies, Regulations, and Societal Well-being in Europe; Leylekian, L.; Covrig, A.; Maximova, A., Eds.; Springer International Publishing: Cham, 2022; pp. 117–139. 337 doi:10.1007/978-3-030-91194-2_5
10 Centracchio, F.; Burghignoli, L.; Iemma, U. Multiobjective optimisation of flight paths for noise level mitigation and sound quality improvement. Noise Mapping 2021, 8, 268–280. doi:doi:10.1515/noise-2021-0022
11 Iemma, U.; Pisi Vitagliano, F.; Centracchio, F. Multi-objective design optimization of sustainable commercial aircraft: performance and costs. International Journal of Sustainable Engineering 2016
12 Iemma, U.; Pisi Vitagliano, F.; Centracchio, F. A multi-objective design optimisation of eco-friendly aircraft: the impact of noise fees on airplanes sustainable development. International Journal of Sustainable Engineering 2017
13 Centracchio, F.; Rossetti, M.; Iemma, U. Approach to the Weight Estimation in the Conceptual Design of Hybrid-Electric-Powered Unconventional Regional Aircraft. Journal of Advanced Transportation 2018, 2018. doi:10.1155/2018/6320197
14 “GasTurb 13: Design and Off-Design Performance of Gas Turbines”, www.gasturb.com, Aachen, Germany, 2012
15 Kurzke, J and Halliwell, I. Propulsion and power: an exploration of gas turbine performance modeling. Cham, Switzerland: Springer international publishing, 2018.
16 Compressor and Turbine Maps for Gas Turbine Performance Computer Programs Issue 3, Tech. rep., GasTurb GmbH, 2021.
17 Schäffer, B., Bertsch, L., LeGriffon, I., Heusser, A., Lavandier, C., Pieren, R., Evaluation of flyover auralizations of today's and future long-range aircraft concepts, InterNoise2022, Glasgow, UK, August 2022
18 M.J.T. Smith: Aircraft Noise, Cambridge Aerospace Series, ISBN 0-521-33186-2, 1989